

Material Issues in AMOLED

Jong Hyuk Lee, Chang Ho Lee and Sung Chul Kim
*Samsung Mobile Display, San #24 Nongseo-Dong, Giheung-Gu, Yongin-City,
Gyunggi-Do, Korea 446-711*

1. Introduction

Since the first mass production of AMOLED (active matrix organic light emitting diode) for mobile display in 2007, many companies have dived into the market for mobile phones and the other portable displays based on extraordinary image qualities of AMOLED. In a mass production point of view, small-sized AMOLED almost attained a stage of technological maturity. However, it still needs some more improvements in terms of materials for lower power consumption, longer life time of AMOLED. Besides outstanding market expansion of AMOLED in mobile applications, AMOLED also can bring us new displays that are only shown in some SF movies, such as paper-thin, foldable, bendable and transparent displays. In terms of power consumption, AMOLED is intrinsically superior to LCD, where the backlight should be always "on". If we consider that the on-ratio is usually less than 30% in most TV broadcastings, a big advantage exists for AMOLED because AMOLED turn on the light for each pixel individually. Moreover, AMOLED still have plenty of rooms to further reduce power consumption. Although low power consumption is the reason why AMOLED is a better choice for portable devices, recent trend of green business require consuming lower power for brighter display. In order to meet those stringent requirements, new materials with high efficiency and optimization of AMOLED device structure is necessary. This article reviews current material issues of AMOLED for general application and for unique application such as transparent and bendable displays.

2. Organic material issues of amoled

2.1 Materials for hole transporting

Since the first report of multi-layered OLEDs, many studies have focused on improving device efficiency and enhancing the durability of OLEDs. Development of new materials for improving device performance such as device driving voltage, efficiency, and life-time is one of the major research subjects in the OLED research area. And there have been lots of progress in performance characteristics. Despite much improved device performance, an insufficient life-time remains one of the primary issues limiting the wide-spread commercial use of OLED. Life-time property is a major obstacle in the competing with liquid crystal display (LCD) as flat panel displays and, life-time related image sticking is an emerging issue of OLED operation.

For the fabrication of highly stable OLEDs, specific optical and electronic properties, such as fluorescence, energy levels, charge mobility etc, and high morphologic stability are required [1-4]. The electrochemical stability of materials used in OLED is very important to improve the device properties. Also, the thermal stability of hole-transporting material is one of the significant factors of the device durability. Under thermal stress, most organic glass transition materials tend to turn into the thermodynamically stable crystalline state, which leads to device failure [5, 6]. It is known that an amorphous thin film with a high glass transition temperature (T_g) is more stable to heat damage [7-11]. In general, high thermal stability, especially high T_g above 100 °C, good hole transporting ability, and excellent film formability are essentially needed for the hole-transporting materials. Various triarylamine derivatives have been utilized as hole-transporting materials (HTMs) because of their good film forming capabilities as well as good hole-transporting abilities [3, 12-13].

The radical cation is one of important reactive intermediate in organic molecules and it can be obtained by loss of single electron from neutral molecules. The chemical structures of common radical cation species are shown in Fig. 1.

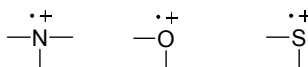
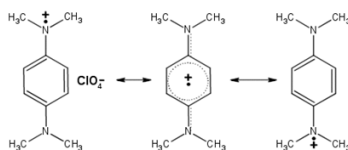


Fig. 1. The common radical cation species

Both hole and charge are not necessary to be localized together on one atom and they can be delocalized over the whole molecule. In fact, the delocalization of the unpaired electron in conjugated system can lead to stable radical cations such as the Wurster salt. This compound is isolable and the chemical structure including its resonance forms are shown in Scheme 1. Aryl amine moieties are thought to be a main core structure in HTMs because amine atom is relatively easy to lose one electron and the resulting radical cation can be stabilized by resonance effect of adjacent aryl substituent. It is worth to note that the Wurster salt mentioned above is stabilized by two factors. One is a resonance effect by aryl substituents and the other is stabilized by counter ion, perchlorate.

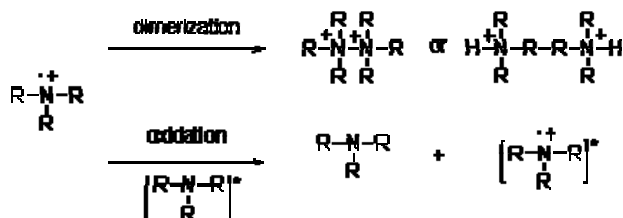


Scheme 1. The possible resonance forms of Wurster salt

However, there is no such stabilization by counter anion in OLED devices. The stability of radical cation mainly depends on its adjacent substituent. Therefore the HTMs stabilized by their substituents are one of important factors to improve the OLED performance.

There are several factors contributing to the stability of radicals. Those are hyperconjugation, resonance, hybridization, captodative effect, and steric effect [24]. Among them resonance and steric effect are important in aryl aminyl radical cations. These aminyl radical cations can be reactive and there are many possible reactions such as fragmentation, dimerization,

disproportionation, and, oxidation. However, the first three reactions are not favorable in OLED device because these give rise to change of the original HTMs via formation or cleavage of σ bond. It is thought to be one of plausible reasons for OLED degradation. However, the oxidation is desirable in OLED device because this single electron transfer process between adjacent molecules results in a hole-transporting process, a fundamental reaction of HTMs. Fragmentation and disproportionation reaction is relatively less important in solid state because the interactions between each radical cations are small but the interactions between a molecule and solvent are strong in solution. In contrast, the dimerization and the oxidation reaction are more important in solid state owing to their strong interaction between radical cation each other. The following Scheme 2 summarizes the important reactions in OLED device.



Scheme 2. Dimerization vs oxidation reaction

Therefore HTMs have to be modified to increase the stability of aminyl radical cation which can result in minimizing the cleavage of σ bond in molecules. Furthermore resonance effect and steric factor have to be considered to minimize the dimerization reaction in solid state. Recently, considerable efforts have been devoted to the development of new amorphous triaryl amines possessing high morphologic stability [14-20]. We have already reported that the device employing thermally stable hole-transporting materials showed high efficiencies [21, 22]. However, it is thought that these hole-transporting materials cannot meet high efficiency and long lifetime simultaneously. Therefore, we will discuss how to modify the structure of HTMs in order to increase their radical cationic stabilities. In addition, device performance with these modified molecules will be discussed.

2.1.1 Physical properties of hole transporting materials

Tested molecules having hole-transporting properties are shown in Fig. 2.

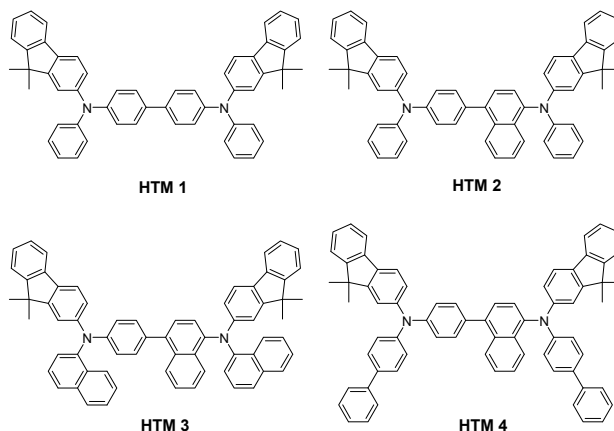
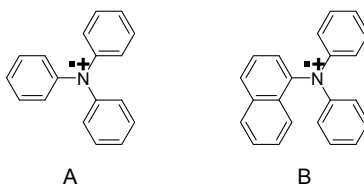


Fig. 2. Hole-transporting materials

Absorption spectra were measured with a HITACHI U-3000 UV spectrophotometer. ^1H NMR and ^{13}C NMR spectra were recorded with a JEOL JNM-ECP 400 FT NMR spectrometer. Differential scanning calorimetry (DSC) was performed on a TA Instruments, DSC-2910 unit using a heating rate of $10\text{ }^\circ\text{C}/\text{min}$ and a cooling rate of $40\text{ }^\circ\text{C}/\text{min}$. Samples were scanned from 30 to $300\text{ }^\circ\text{C}$, cooled to $0\text{ }^\circ\text{C}$, and then scanned again from 30 to $300\text{ }^\circ\text{C}$. The glass transition temperatures (T_g) were determined from the second heating scan. Thermogravimetric analysis (TGA) was undertaken on a TA instrument, TGA-2050. The thermal stability of phenyl-naphthylamine derivatives was determined under a nitrogen atmosphere, by measuring weight loss while heating at a rate of $20\text{ }^\circ\text{C}/\text{min}$. The results are summarized in Table 1 along with literature data of common hole-transporting materials for comparison. The ionization potentials (IPs) of materials used in device fabrication were determined by ultraviolet photoelectron spectroscopy (UPS) (Riken Keiki, AC-2) using the samples prepared by PMMA polymer binder on glass and the energy levels of lowest unoccupied orbital (LUMO) were approximately defined as differences between IPs and long wavelength cutoffs of the absorption spectra of 0.2 mM CH_2Cl_2 solution.

As mentioned before, a radical cation of **HTM 2** is more stable than that of **HTM 1** by two factors. As shown in structure A and B, the naphthyl amine radical cation B is preferred because it has two more resonance forms than cation A. It is well known that molecules having more resonance form are more stable. In addition, cation B can be stabilized further by steric effect. A bulky naphthyl moiety which is bigger than phenyl moiety can retard dimerization of radical cations.



The thermal stability data of these three phenyl-naphthylamine derivatives, **HTM 2-4**, were investigated by differential scanning calorimetry and thermogravimetric analysis; the

results are summarized in Table 1 with the well-known hole-transporting material **HTM 1** for comparison. As shown in Table 1, all three phenyl-naphthyl-diamine-cored HTMs (**HTM 2-4**) have higher value of T_g relative to their biphenyl-diamine analog **HTM 1**, proofing the high morphologic stability of the amorphous phase in a deposited film, which is a prerequisite for the application in organic electroluminescent devices.

According to Shirota [1], a non-planar molecular structure preventing easy packing of molecules and an increased number of conformers in the molecule are preconditions in the design and synthesis of amorphous molecular glasses. Glass formation is enhanced by incorporation of bulky substituents. The incorporation of bulky substituents also hinders translational, rotational and vibrational motions of molecules, leading to an increase in the T_g . We attribute to the increase in the morphological stability of the biphenyl-based material to the presence of naphthalene substituents at the central phenyl-naphthyl core, which may hinder the crystallization process. It is important that OLEDs be constructed from materials having a relatively high value of T_g to avoid problems associated with crystallization, which leads to device degradation.

The HOMO and LUMO levels of these phenyl-naphthyl-diamine derivatives are also listed in Table 1. The HOMO was determined using a photoelectron spectrometer, while LUMO was calculated based on the HOMO energy level and the lowest energy absorption edge of the UV absorption spectrum. The HOMO and LUMO levels of these compounds were measured at ca. 5.40 - 5.45 eV and 2.43 - 2.53 eV, respectively.

Compounds	T_d^a (°C)	T_g^b (°C)	T_m^b (°C)	T_c^b (°C)	λ_{max}^c (nm)	HOMO ^d (eV)	LUMO ^e (eV)
HTM 1	380	121	264	NA	360	5.40	2.38
HTM 2	395	159	296	NA	342	5.40	2.43
HTM 3	430	167	225	NA	355	5.45	2.53
HTM 4	423	174	255	NA	353	5.45	2.48

^a Obtained from TGA measurement. ^b Obtained from DSC measurement. ^c Measured in CH_2Cl_2 solution. ^d Determined by ultraviolet photoelectron spectroscopy (UPS). ^e Calculated based on the HOMO level and the lowest energy absorption edge of the UV spectrum.

Table 1. Physical properties of the phenyl-naphthyl-diamine derivatives and biphenyl-diamine derivative **HTM 1**

2.1.2 Device fabrication and characteristics

Prior to device fabrication, ITO with a resistance of $15 \Omega/\square$ on glass was patterned as an active area of 4mm^2 ($2\text{mm} \times 2\text{mm}$) square. The substrates were cleaned by sonication in deionized water, boiled in isopropylalcohol for 20 min, and dried with nitrogen. Finally, the substrates were treated with UV/ozone for 20 min. Organic layers were deposited sequentially by thermal evaporation from resistively heated alumina crucibles onto the substrate at a rate of $0.5 - 1.0 \text{ \AA}/\text{sec}$ in the organic chamber. The base pressure at room temperature was 3×10^{-6} Torr. The deposition rate was controlled using a ULVAC crystal monitor that was located near the substrate. After organic film deposition, the substrate was transferred to another chamber maintaining the base pressure of 3×10^{-6} Torr. Before the deposition of metal cathode, LiF was deposited onto the organic layers with the thickness of

10 Å. A high-purity aluminum cathode was deposited at a rate of 4–8 Å/sec with the thickness of 3000 Å as the top layer. After the metal chamber was vented with N₂ gas, the device was immediately transferred to an N₂-filled glove-box upon fabrication. A thin bead of epoxy adhesive was applied from a syringe around the edge of a clean cover glass. To complete the package, a clean cover glass was placed on the top of the device. The epoxy resin was cured under intense UV radiation for 5 min. The current–voltage characteristics of the encapsulated devices were measured on a programmable electrometer having current and voltage sources, Source Measure Unit, model 238, (Keithley). The luminance and EL spectra were measured with a PR650 system (Photo Research). The current–voltage, EL spectra and luminance measurements were carried out in air at room temperature. Only light emitting from the front face of the OLED was collected and used in subsequent efficiency calculations.

To evaluate hole-transporting ability of newly synthesized phenylnaphthylidiamine derivative **HTM 2**, we fabricated the hole-dominant device using **HTM 2** as a hole-transporting material with structures as follows: ITO/2-TNATA/**HTM 2**/EML/Al (device II). On ITO substrate, 4',4''-tris(*N*-(naphth-2-yl)-*N*-phenyl-amino)tri-phenylamine (2-TNATA) was previously deposited as a hole-injecting material. IDE 215 doped with 3 % of IDE 118 (host and dopant materials by Idemitsu Co., LTD) was used as blue emitting layer.

		Al (3000 Å)	Al (3000 Å)
		EIL (10 Å)	EIL (10 Å)
Al (1500 Å)	Al (1500 Å)	ETL (250 Å)	ETL (250 Å)
EML (300 Å)	EML (300 Å)	EML (300 Å)	EML (300 Å)
HTM 1 (500 Å)	HTM 2 (500 Å)	HTM 1 (300 Å)	HTM 2-4 (300 Å)
HIL (500 Å)	HIL (500 Å)	HIL (600 Å)	HIL (600 Å)
ITO	ITO	ITO	ITO
Device I	Device II	Device III	Device IV-VI

Fig. 4. Structures of EL devices used in this study

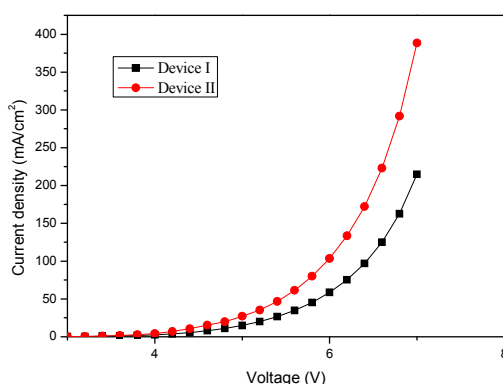


Fig. 5. Current density-applied voltage characteristics of device I and II

A reference device I composed of **HTM 1** as a hole-transporting material with the same thickness was also constructed for comparison (Fig. 4). The current-voltage (I-V) characteristics of the devices are shown in Fig. 5. The current density of the device II prepared with **HTL 2** is almost twice higher than that of the reference device I (103.4 mA/cm² vs 58.5 mA/cm² at 6 V). These outcomes showed that the hole-transporting ability of a phenylnaphthylamine-cored **HTM 2** was highly improved than that of biphenylamine-cored **HTL 1** due to its more resonance form in the radical cation as well as the steric effect of a naphthyl moiety resulting in efficient carrier transportation.

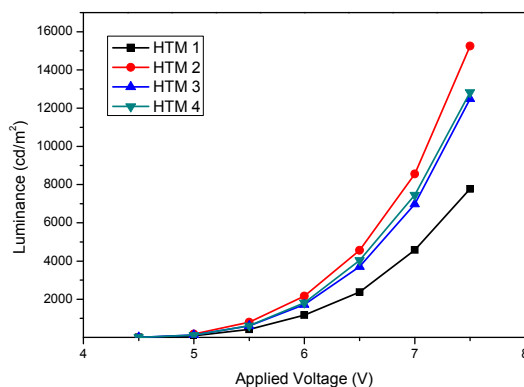


Fig. 6. Luminance-applied voltage characteristics of devices III-VI.

We also expected the stability of the phenylnaphthyl core is better than that of the biphenyl core since it has more resonance structure and higher radical stability. Three EL devices: ITO/2-TNATA/**HTM 2**/EML/Alq₃/LiF/Al (device IV), ITO/2-TNATA/**HTM 3**/EML/Alq₃/LiF/Al (device V), and ITO/2-TNATA/**HTM 4**/EML/Alq₃/LiF/Al (device VI), were fabricated in order to estimate their suitabilities as a hole transporting material in comparison with the reference device; ITO/2-TNATA/**HTM 1**/EML/Alq₃/LiF/Al (device III). The structures of EL devices are shown in Fig. 4. Fig. 6 shows the luminance and the applied voltage characteristics in the four devices. The luminance of the device IV reached 4,561 cd/m² at 6.5V.

Surprisingly, the devices IV-VI with **HTM 2-4** as a hole-transporting material showed a significant enhancement of the luminous efficiency compared to reference device III. The luminous efficiency of the device IV is about 40% higher than that of the device III. The luminous efficiencies of other two devices were also higher than that of the device III. The luminous efficiencies of the device IV-VI with **HTM 2-4** were 8.52, 7.98 and 7.50 cd/A, respectively. Table 2 shows the EL performances of all devices at 6.5V and Fig. 7 shows the current efficiency-applied voltage characteristics.

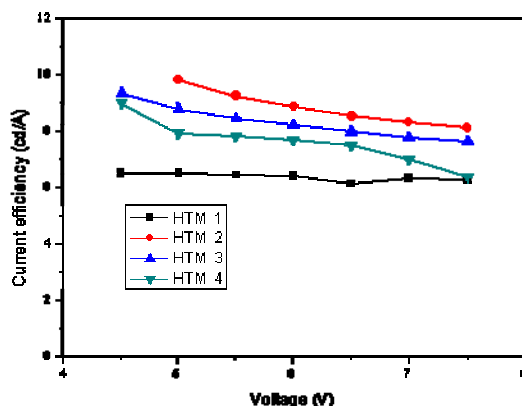


Fig. 7. Current efficiency–applied voltage characteristics of devices III-VI.

Device	Current density (mA/cm ²)	Luminance (cd/m ²)	Current efficiency (cd/A)
Device III	39.01	2383.2	6.11
Device IV	53.54	4561.6	8.52
Device V	46.48	3708.9	7.98
Device VI	53.87	4041.0	7.50

Table 2. EL performance of four devices III-VI at 6.5V

As shown in Table 2, the devices IV-VI using **HTM 2-4** as a hole-transporting material showed remarkable current density and current efficiency performance compared to the reference device III. Fig. 6 shows the devices III needs higher electric power than the devices IV-VI at the same luminance. In other words, it is thought that phenyl-naphthyl-diamine derivatives **HTM 2-4** have superior hole-transporting abilities than biphenyl-diamine derivative **HTM 1**. As we mentioned before, these high performances of the devices IV-VI, using phenyl-naphthyl-diamine derivatives might be attributed to the more efficient hole transportation and higher T_g of those compounds compared to that of biphenyl-diamine derivative.

Fig. 8 shows the life-time characteristics of the device IV and the reference device III. The life-time of the device IV is about two times longer than that of the standard device III within the measured current density, indicating more effective recombination at the emitting layer of device IV. These results indicated that phenyl-naphthyl-diamine derivatives have higher hole-transporting abilities and stabilities toward electric current than that of biphenyl-diamine derivative.

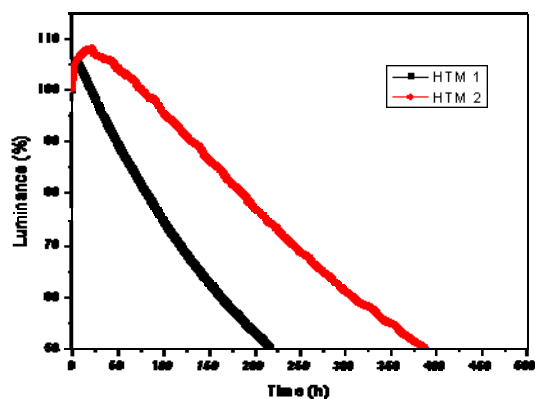


Fig. 8. The life-time characteristics of the two devices at 100mA/cm²; device III (■), device IV (●)

Consequently, hole transporting materials having naphthalene moiety are more stable in radical cation state because of more resonance form and sterically more favored than that of phenyl moiety because of retardation of dimerization reaction. These two factors can contribute to the enhancement of the hole transporting ability resulting in better OLED performance. The device of fluorescent blue OLED using phenyl naphthyl diamines as the hole-transporting layer have much better overall EL performance and longer life-time than the reference device with biphenyl diamine layer.

2.2 Materials for electron transporting

Above mentioned, although OLEDs have shown high brightness and vivid color, long-term stability and image sticking remains a critical issue for practical applications. Device degradation is also largely attributed to the delamination between different layers and the crystallization of organic materials due to electrochemical reaction on interfaces. In general, degradation in OLEDs essentially appears in the form of a decrease in device luminance with time. The decrease in luminance can proceed through three independent and visually distinct modes. These modes are referred as (i) dark-spot degradation, (ii) catastrophic failure, and (iii) intrinsic degradation [23]. These well known degradation mechanism is related with intrinsic material properties as well as device structure.

Recently, it was elucidated that dipole moment of ETM (electron transport material) could be an important factor of initial luminance decrease in OLED. It is well known that luminance decrease at initial phase is a main reason for image sticking. In this chapter, we will focus on electron transporting material-dependent life-time pattern and found the relationship between dipole moment of electron transporting material and initial life-time tendency. It is explained how dipole moment of ETM affected initial luminance decrease in OLED [24-26].

To elucidate a cause of luminance decrease, it has been designed and synthesized a series of ETMs with different value of dipole moment and evaluated the initial life-time of the OLED device using them as ETM.

2.2.1 Dipole moment of electron transporting materials

Dipole moment values for each ETM were calculated by using GAUSSIAN 03 program package. We generated the optimized geometric structure by means of time-dependent density functional theory (TD-DFT) [27],[28] and each dipole moment value was included in the calculation summary. Dipole moments of ETMs were enlisted in Fig. 9 (ADN (Anthracene dinaphthalene) derivatives), Fig. 10 (Phenanthroline derivatives) and there were dipole moment differences among the ETMs according to the arrangement of heteroatom in the molecules. The ETMs were designed in order to minimize the effect of molecular size (Induced dipole-induced dipole interaction or London force) and dipole-dipole interaction is predominant intermolecular force among them.

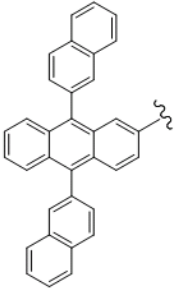
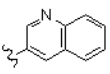
Structure	Name	
	Dipole moment (Debye)	
		ET1
		ET2
		ET3
		ET4
		3.4774
		2.9772
		2.5572
		2.0040

Fig. 9. Molecular structure and calculated dipole moment of ADN series ETMs

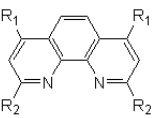
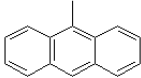
		Name
		Dipole moment (Debye)
$R_1 =$ 	$R_2 =$ 	ET5 3.6353
$R_1 =$ 	$R_2 =$ 	ET6 3.1120
$R_1 =$ 	$R_2 =$ CH ₃	ET7 2.9257
$R_1 =$ H	$R_2 =$ 	ET8 2.1860

Fig. 10. Molecular structure and calculated dipole moment of Phenanthroline series ETMs

2.2.2 Device fabrication and characteristics

All OLEDs were fabricated on indium tin oxide precoated onto glass substrate. Organic layers were vacuum deposited via thermal evaporation in the high-vacuum chamber. Fig. 11 shows the structure of blue OLED device and its energy diagram. The thickness and materials of each layer are same for fabricated devices except ETMs to eliminate another possible luminance attenuating factor.

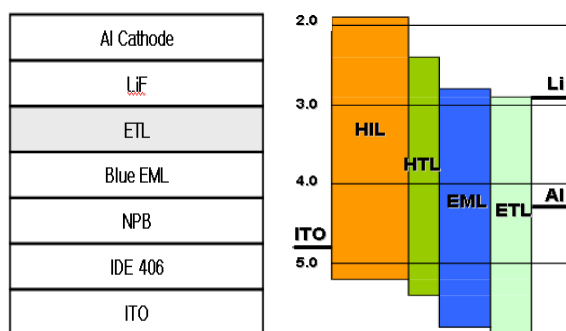


Fig. 11. Blue OLED structure and Energy diagram

The IVL (current density, applied voltage, luminance) characteristics of OLEDs were measured using a Photo Research Inc. PR-650 spectrometer. The operational life-time characteristics were determined from a series of measurements of changes in luminance and drive voltage as function of time under DC driving conditions.

Devices performance properties depended on ETMs and their ability to transport electron [29]. Fig. 12 and Fig. 13 showed I-V and L-Efficiency characteristics of ADN series ETMs, respectively. Regardless of dipole moment differences, device performances depended on the electron transporting ability of the hetero-aromatic rings attached to ADN backbone, and similar property tendency was observed when we applied those hetero-aromatic rings to another framework before. **ET4** (quinoline moiety) gave the best electron transporting performance, but **ET2** (iso-quinoline) showed poor electron transporting ability. In spite of different electronic structures of hetero-aromatic rings, Pyrimidine(**ET1**) and pyridine(**ET3**) moieties exhibited similar properties.

Similar to the results of the ADN series ETMs, it was difficult to explain the result in dipole moment aspect, and device performance characteristics mainly due to the property of phenanthroline stacking. **ET7** and **ET8** are simple structure with minimum appendages and almost flat 3-D structure, so they can be effectively stacked through π - π interaction in deposited layer. On the other hand, relatively bulky side aromatic rings obstruct stacking of phenanthroline moiety. It is well known that π - π stacking among ETMs in deposited layer can enhance electron transporting ability, and that is corresponded with the results of the phenanthroline ETMs [30].

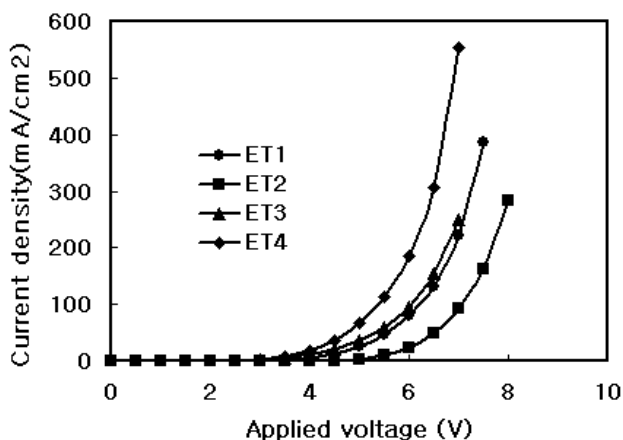


Fig. 12. Voltage-Current curve of ADN series ETMs

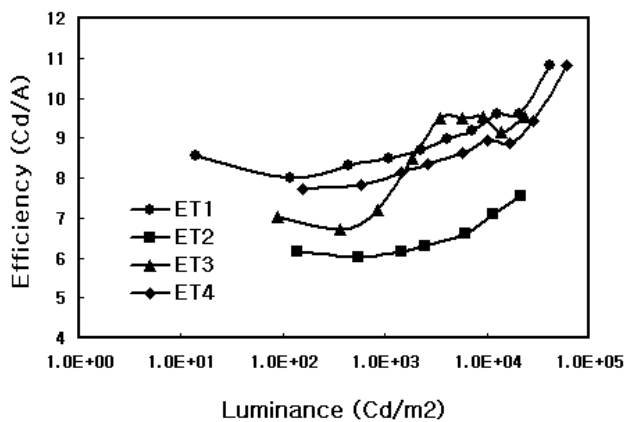


Fig. 13. Luminance-Current efficiency curve of ADN series ETMs

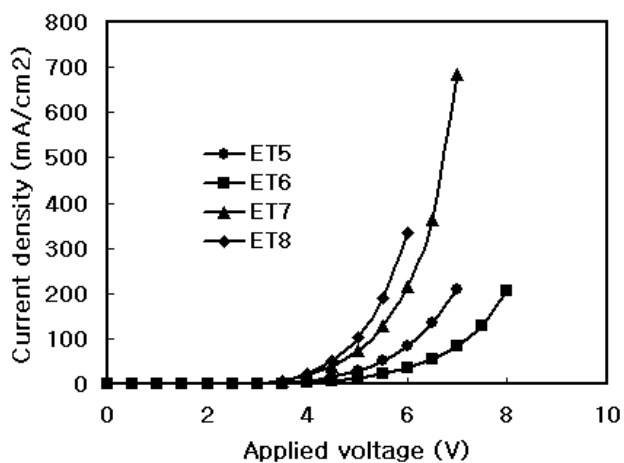


Fig. 14. Voltage-Current curve of Phenanthroline series ETMs

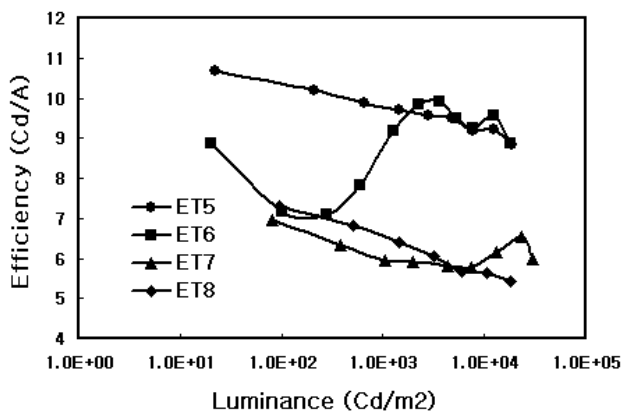


Fig. 15. Luminance-Current efficiency curve of Phenanthroline series ETMs

2.2.3 Analysis of Initial Luminance Decrease

Contrary to the results of performance property, initial phase tendencies of life-time were well corresponded with the dipole moment values. As showed in Fig. 16, the rate of an initial luminance was decreased in the order of **ET1**, **ET2**, **ET3**, and **ET4**, which is contrary to the direction of the dipole moment increase in Fig. 9. **ET1** that can form a robust deposited layer through strong dipole-dipole interactions showed moderate luminance decrease tendency. It can stack regularly in order to form intermolecular network through localized charge distribution in the molecules. It is supposed that an electrically polarized material located under electric field is torqued by an applied electric force and tends to rotate (Fig 17).

When a high electric field is applied, if a material has great dipole moment, phase transformation is difficult to occur in the layer owing to strong intermolecular interactions among deposited molecules (Fig 18a). On the other side, because a low dipole moment material (**ET4**) could not have strong intermolecular force, it cannot stack in compact manner. So it forms less tight layer than materials with strong dipole moment. As depicted in Fig. 18b, deposited molecules rearrange along the electric field or bond strain could be generated in the molecule, and if there is a weak chemical bond, that could be broken when high electric field is applied. In the event, a device composed of small dipole moment ETM showed a steep slope in time-luminance graph at initial phase.

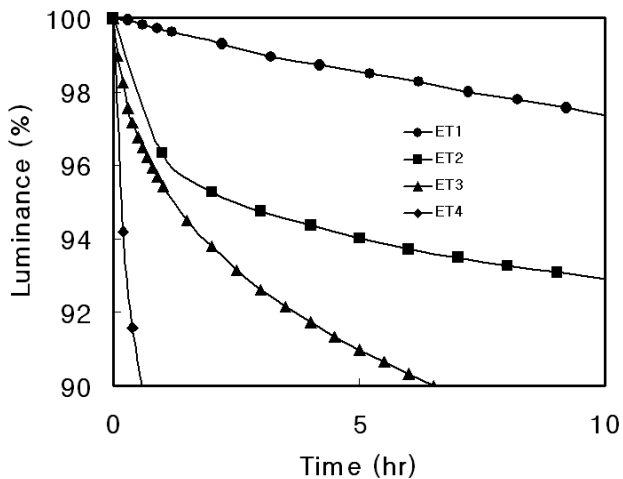


Fig. 16. Initial luminance decrease tendency of devices with ADN series ETMs at 100mA/cm².

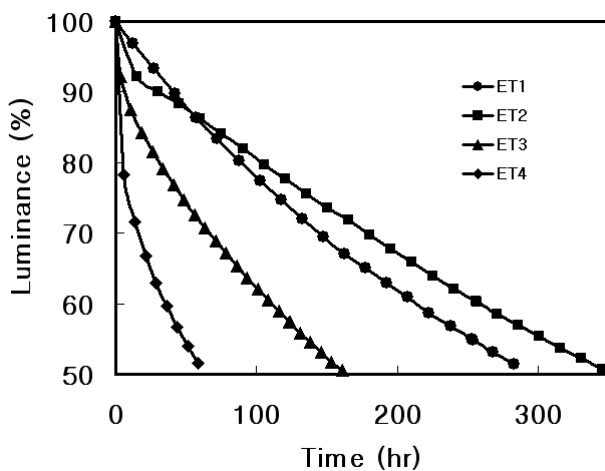


Fig. 16. Life time (half-life) tendency of devices with ADN series ETMs at 100mA/cm²

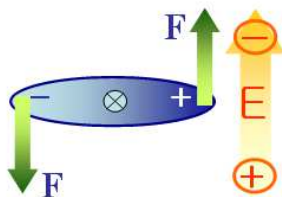


Fig. 17. Behavior of a polarized molecule when electric field is applied

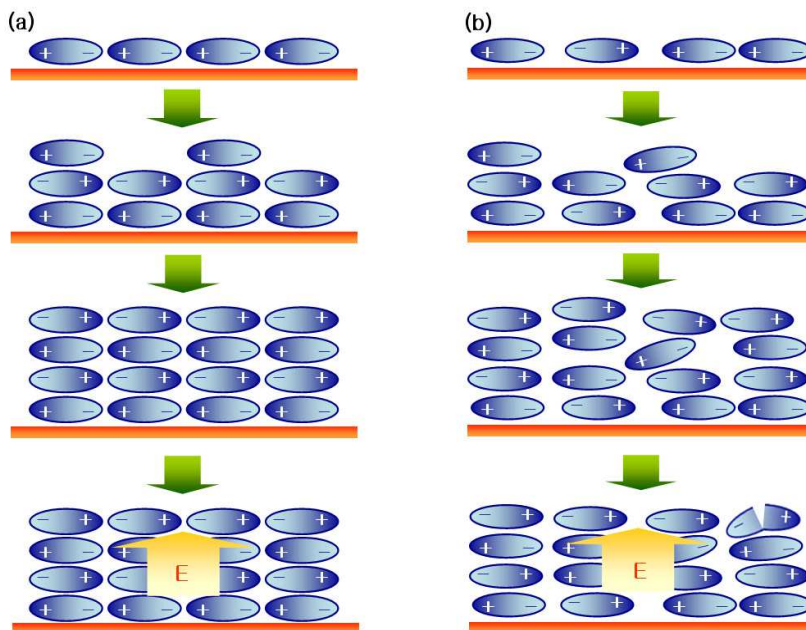


Fig. 18. Schematic descriptions of layer stacking and behavior pattern of polarized molecules under electric field. (a) Material with great dipole moment (b) Material with small dipole moment

Pattern of half-life was similar to that of initial phase, but there must be another factor that could affect life-time. There are some assumed mechanisms for luminance decrease or device degradation [31],[32]. For example, degradation of the interface between deposited layers, shift of exciton recombination zone from emitting layer, intrinsically weak chemical bond of used materials and there must be a lot of possible degradation mechanism we could not conceive.

For the test result (Fig. 16), **ET2** showed dramatic luminance decrease in the initial stage, but after initial rearrangement of molecules in the layer, luminance decreased in a moderate manner. On the other hand, luminance decrease rate of **ET1** device was almost constant over all in operation.

Same luminance decrease tendency was observed in phenanthroline series ETMs. Fig. 19 showed the initial luminance of the devices decreased according to the dipole moment order of ETMs, but half-life in Fig. 20 showed a little different degradation order like the case of the ADN series ETMs. **ET6** and **ET8** gave moderate overall life-time graph, and, **ET5** and **ET7** showed Different stacking pattern caused by dipole moment differences could affect density of deposited layer. If the deposited molecules can interact more tightly each other, density of the deposited layer is greater than less tightly interacting one. Actually, density of deposited layer could be influenced by molecular shape and dipole moment. And to avoid ambiguity from structural differences, we measured densities of **ET1** and **ET3** using XRD

[33] because these two materials are spatially same structure except C-H and N. Densities of **ET1** and **ET3** are 1.25 g/cm^3 and 1.21 g/cm^3 respectively, and this result reflects dipole moment differences. Density differences of the deposited layers also provided a clue for elucidating effect of dipole moment on the pattern of luminance decrease at initial phase.

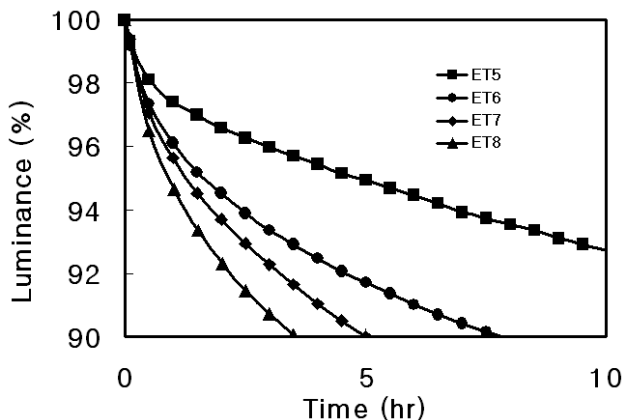


Fig. 19. Initial luminance decrease tendency of devices with Phenanthroline series ETMs at 100mA/cm^2 relatively rapid degradation appearance.

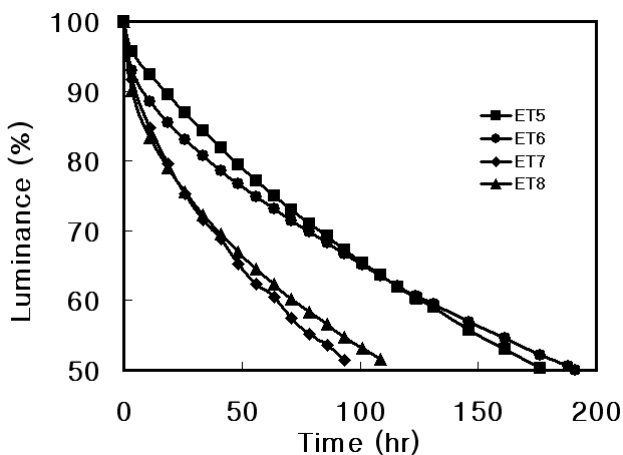


Fig. 20. Life time (half-life) tendency of devices with Phenanthroline series ETMs at 100mA/cm^2

It is concluded that the life-time properties at initial phase were controlled by dipole moment differences of ETMs and great dipole moment materials can enhance initial luminance properties by means of strong dipole-dipole interactions among the molecules. In near future, it is expected to find out a general mechanism of dipole moment effect on life-time.

Thank You for previewing this eBook

You can read the full version of this eBook in different formats:

- HTML (Free /Available to everyone)
- PDF / TXT (Available to V.I.P. members. Free Standard members can access up to 5 PDF/TXT eBooks per month each month)
- Epub & Mobipocket (Exclusive to V.I.P. members)

To download this full book, simply select the format you desire below

